
Structure and properties of bivalent nickel and copper complexes with pyrazine-amide-thioether coordination: Stabilization of trivalent nickel

Akhilesh Kumar Singh and Rabindranath Mukherjee*

Department of Chemistry, Indian Institute of Technology Kanpur, Kanpur 208 016, India

E-mail: rnm@iitk.ac.in; Fax: +91-512-2597437.

Electronic Supporting Information (ESI)

Fig. S1. UV/VIS spectrum (in CH₂Cl₂) of [Cu^{II}(bpzctb)] (**2**).

Fig. S2. Reciprocal molar susceptibility *vs* temperature plots for (a) [Ni^{II}(bpzctb)] (**1**) and (b) [Cu^{II}(bpzctb)] (**2**).

Fig. S3. EPR spectrum of a polycrystalline sample of [Cu^{II}(bpzctb)] (**2**) at 300 K.

Fig. S4. EPR spectrum of [Ni^{III}(bpzctb)]⁺ (coulometrically generated in CH₂Cl₂) at 120 K.

Fig. S5. UV/VIS spectrum of [Ni^{III}(bpctb)]⁺ (coulometrically generated in CH₂Cl₂).

Fig. S6. EPR spectrum of [Ni^{III}(bpctb)]⁺ (coulometrically generated in CH₂Cl₂) at 300 K.

Fig. S7. EPR spectrum of [Ni^{III}(bpctb)]⁺ (coulometrically generated in CH₂Cl₂) at 120 K.

Fig. S1. UV/VIS spectrum (in CH_2Cl_2) of $[\text{Cu}^{\text{II}}(\text{bpzctb})]$ (2).

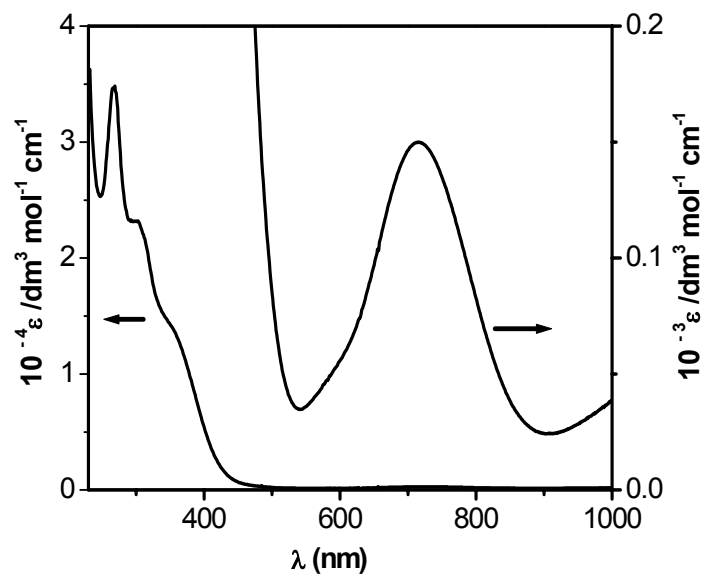
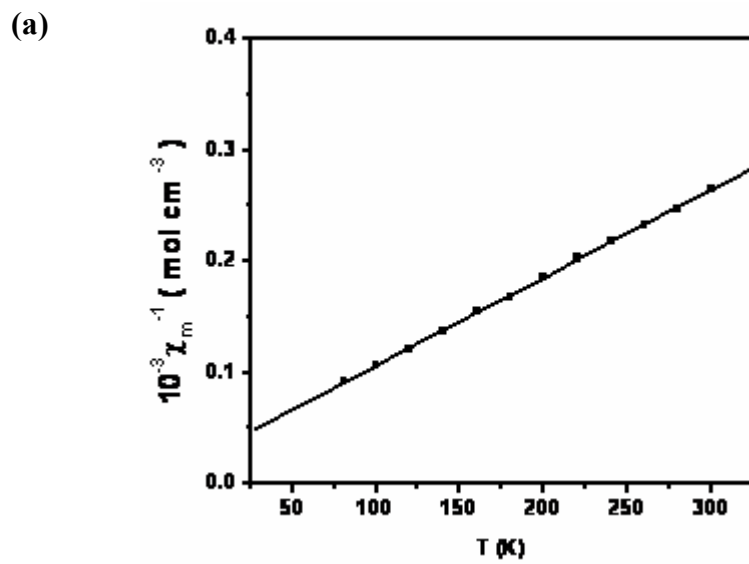


Fig. S2. Reciprocal molar susceptibility vs. temperature plots for (a) $[\text{Ni}^{\text{II}}(\text{bpzctb})]$ (1) and (b) $[\text{Cu}^{\text{II}}(\text{bpzctb})]$ (2).



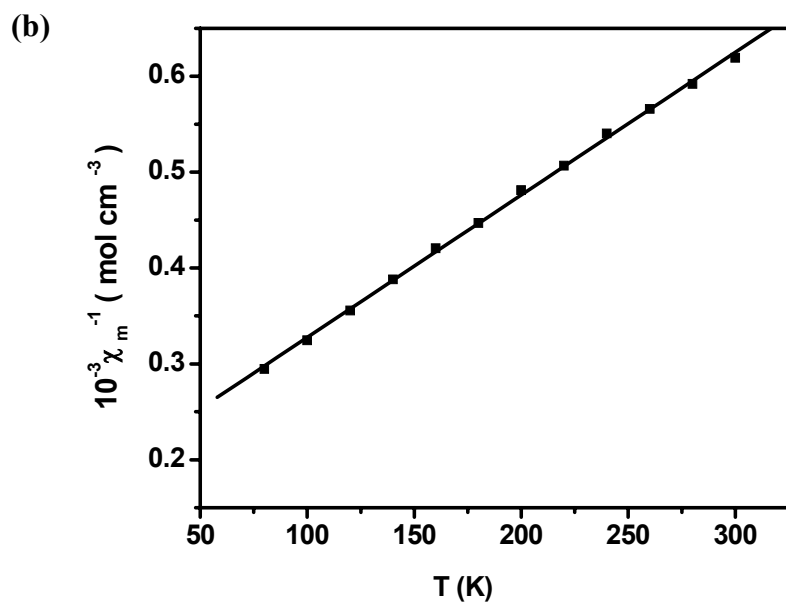


Fig. S3. EPR spectrum of a polycrystalline sample of $[\text{Cu}^{\text{II}}(\text{bpzctb})]$ (**2**) at 300 K.

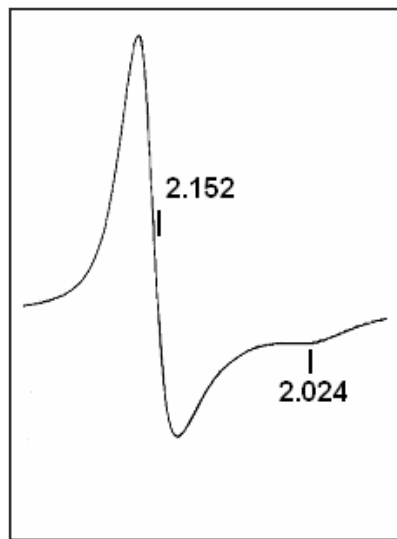


Fig. S4. EPR spectrum of $[\text{Ni}^{\text{III}}(\text{bpzctb})]^+$ (coulometrically generated in CH_2Cl_2) at 120 K

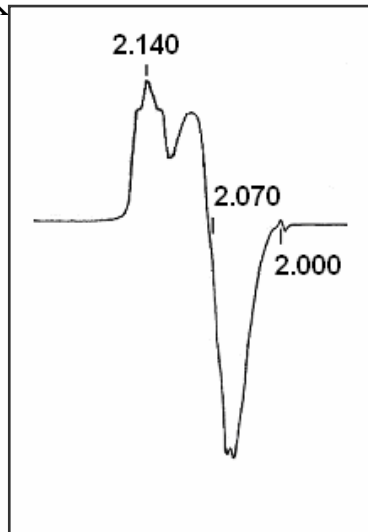


Fig. S5. UV-vis spectrum of $[\text{Ni}^{\text{III}}(\text{bpctb})]^+$ (coulometrically generated in CH_2Cl_2).

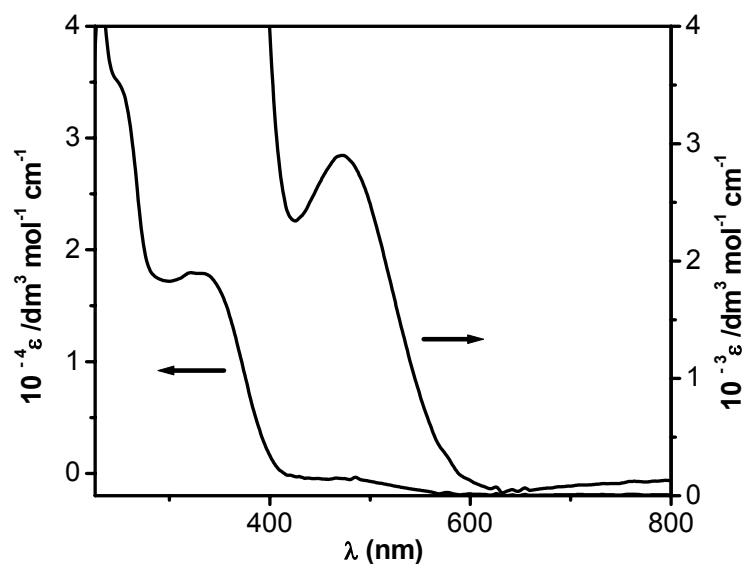


Fig. S6. EPR spectrum of $[\text{Ni}^{\text{III}}(\text{bpctb})]^+$ (coulometrically generated in CH_2Cl_2) at 300 K.

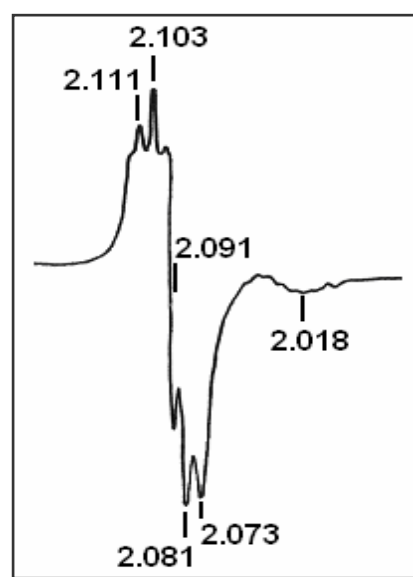


Fig. S7. EPR spectrum of $[\text{Ni}^{\text{III}}(\text{bpctb})]^+$ (coulometrically generated in CH_2Cl_2) at 120 K.

